On the classification of temporal lobe epilepsy using MR image appearance

S. Duchesne, N. Bernasconi, A. Bernasconi and D.L. Collins

Abstract— **Classification of neurological diseases based on image characteristics often requires extensive modeling and user intervention. While other techniques concentrate on specific structures, the novelty of the method presented here resides in its analysis of the grey-level apperance of large, non-specific Volumes of Interest (VOI) from T1 MRI data. No manual intervention is required other than the selection of the VOI. This work presents the methodological framework and preliminary results towards our aim of classifying normal subjects and patients with Temporal Lobe Epilepsy (TLE) within the Medial Temporal Lobe. For this purpose, Principal Components Analysis is performed on a set of normal subjects for the creation of a multi-dimensional space representative of a normal population. New data for normal and TLE subjects are projected in this space, under the assumption that the distributions of the projections are not identical and can be used for classification. It is shown that Linear Discriminant Analysis of the eigencoordinates of the projected data can be used to classify normals vs TLE with a 70% accuracy based on only 10 eigenvectors. This results can go up to 100% if all eigenvectors defining the grey-level space are used.**

Keywords— **Magnetic Resonance Imaging, Pattern Classification, Linear Discriminant Analysis, Appearance Models, Principal Components Analysis**

I. Introduction

CLASSIFICATION of neurological diseases based solely on their imaging characteristics is a challenging task for computer vision. Most of the work to date on automated classification of various diseases or disorders such as epilepsy [4], Alzheimer's disease [7], and schizophrenia [13], [10] has been focused on MR image analysis of the hippocampus (HC), a structure which is affected by pathological processes in these diseases. Temporal Lobe Epilepsy (TLE) is characterized by seizures originating in the medial temporal lobes (MTL). TLE is frequently associated with hippocampal atrophy, which has been shown to correspond to neuronal loss and gliosis on histology. On T1-weighted MRI, a hypointense signal is observed within the hippocampus.

Recent observations in animal models [3] and in patients with TLE [1], [2] indicate that the epileptogenic zone is broad, suggesting that the substrate for seizure generation is distributed over a network including several other structures in the MTL. Therefore, we believe it possible to design a classification technique which would use intensity information from a large, non-specific Volume of Interest (VOI) rather than one particular structure such as the HC.

Other works require the segmentation of all structures of interest within the VOI and the identification of relationships between them. In our approach, the appearance of the VOI as a whole is assessed without explicit segmentation.

In this sense, our current work follows the direction of the appearance-based segmentation technique which we proposed in [8]. This segmentation process, inspired by the methods of Cootes et al. [6], models of the intensity characteristics and shape deformations of the VOI are constructed and concatenated into an appearance model for the Volume. The linear modeling employs Principal Components Analysis (PCA) to generate spaces of allowable variations in grey-level intensity and shape deformations. For the purposes of this study, we concentrate on the grey-level characteristics of the VOI, consequent with our research hypothesis that there exists sufficient discriminatory information between intensity distributions of normal and abnormal populations to effectively classify a new subject.

Thus, if one takes the eigenvectors of the linear grey-level model as orthonormal bases spanning an n-dimensional allowable space (where n is the number of voxels present), the distribution of the projection in this space of data from subjects belonging to the training set can be used as a probability function characterizing the type of population present in the training set. A matching statistic can be assigned for grey-level images of a new subject projected in the same space. This similarity measure can be associated with a particular pathological difference between the new subject and the training set. The aim is to derive diagnostic information correlated to a particular Principal Component (PC) or distribution in PCA space.

The goal of our research in this area is thus concerned with the development of an automatic classifer which would serve to identify TLE based solely on grey-level appearance of the MR images. The aim of this paper is to present the methodology for such an application.

II. Methods

A. Creation of multi-dimensional spaces to represent data

As mentioned earlier, the background for this work stems from our work in appearance-based segmentation where a number of PC spaces were created from analysis of a number of VOIs from a training set, as well as their corresponding nonlinear deformation fields.

In this work a space is being created from grey-level PC which could be used to characterize images. The notation employed by Cootes [6] will be closely followed. We start by using an initial set of N *normal* subjects (see section III-B), the Domain Definition set, to form an Allowable Grey Domain (AGD). To make the PCA a zero-mean process, in-

S. Duchesne, N. Bernasconi, A.Bernasconi and D.L. Collins are with the Brain Imaging Center, Montréal Neurological Institute, McGill University, Montréal, Canada. Email: {duchesne,neda,andrea,louis}@bic.mni.mcgill.ca

put Volumes into the analysis are *difference images*. Hence this *difference vector* $\mathbf{g}$ consists of rasterized grey-level data from the original VOI $\mathbf{v}_{\text{subject input}}$ minus the average of all original volumes $\mathbf{v}_{\text{average input}}$:

$$\mathbf{g} = \mathbf{v}_{\text{subject input}} - \mathbf{v}_{\text{average input}} \tag{1}$$

and hence we define $\bar{\mathbf{g}}$ as the arithmetic average of the difference images, or

$$\bar{\mathbf{g}} = \frac{1}{N}\sum_{\mathbf{i=1}}^{\mathbf{n}} \mathbf{v_i} \tag{2}$$

and not the average of the input volumes. In effect, the PCs therefore extracted represent or explain the differences between a subject and the mean of the group. The VOI, albeit not homogeneous, does not exhibit large variability between subjects.

PCA is used to reduce the dimensionality of the grey-level data and generate a linear grey variation model [6]:

$$\mathbf{g} = \bar{\mathbf{g}} + \mathbf{P_g B_g} \tag{3}$$

which allows any grey-level *difference vector* instance $\mathbf{g}$ to be approximated by $\bar{\mathbf{g}}$, the mean normalised grey-level *difference vector*, $\mathbf{P_g}$, the set of orthogonal modes of variation and $\mathbf{B_g}$, the set of grey-level parameters.

In order to know how each principal direction contributes to the description of the total variance of the system, the ratio of relative importance of the eigenvalue λ_k associated with the eigenvector k is used

$$r_k = \frac{\lambda_k}{\Sigma_{j=1}^{p}\lambda_j} \tag{4}$$

where the fraction r_k is the relative importance for eigenvalue λ_k, over the sum of all λ, since p is the total number of eigenvectors. Note that $p = N - 1$ and constitutes the upper bound on the dimensionality of P_g and B_g.

In the aforementioned PCA model, a percentage $f\%$ is selected, such that t eigenvectors are kept which explain this desired level of variance for the system:

$$r_1 + r_2 + ... + r_t > \frac{f}{100} \tag{5}$$

The choice of threshold f will be dependent on the total amount of variation which the model is asked to represent. Statistical methods of finding the optimum number of eigenvectors exist but have not been implemented yet.

We define the Allowable Grey Domain $\mathbf{G}$ as the space of all possible elements expressed by eq. 3, $\forall\ \mathbf{P_g}$, and a restricted version of this space, $\mathbf{G}^*$, such that

$$\mathbf{G}^*_{\mathbf{P_g}} \subset \mathbf{G}_{\mathbf{P_g}} \tag{6}$$

and where the upper bound on the dimensionality of $\mathbf{G}$ is p, as defined above, while the upper bound for $\mathbf{G}^*$ is t, set by choosing the threshold f in eq. 5.

B. Extraction of features of interest and classification

Closely following the notation of Duda et al. [9], we will define two states of nature ω: $\omega_1 = \textit{normal subjects}$ and $\omega_2 = \textit{temporal lobe epileptics}$. Note that normal subjects are part of a control group and are not the same as those belonging to the training or Domain Definition set used to create the AGD.

For the purposes of this work, the *prior* probabilities $p(\omega_1)$ and $p(\omega_2)$ are known since the compositions of the classification data sets will be known exactly (see sec. III). Note that they do not represent the normal incidence rates of TLE in the general population.

MRI data *difference* volumes from each of the two w categories are projected into the Domain $\mathbf{G}^*$ and thus form the eigencoordinate vectors $\chi_{\mathbf{i}}^{\omega}$

$$\chi_{\mathbf{i}}^{\omega} = (\mathbf{V}_{\mathbf{i}}^{\omega})^{\mathbf{t}} * \mathbf{V_g} \tag{7}$$

where $\mathbf{V}_{\mathbf{i}}^{\omega}$ represents the rasterized grey-level vector for each training volume belonging to the two different categories.

A number of possible features can now be calculated on the distribution of these eigencoordinate vectors. The one we will originally base our classification scheme on is the position along the PC axis. We can reasonably assume that it can be represented by a Gaussian distribution, and thus the formulation of our feature vectors $\mathbf{p}$ for each subject i follows easily from eq. 7:

$$\mathbf{p}_{\mathbf{i}}^{\omega} = \chi_{\mathbf{i}}^{\omega} \tag{8}$$

The design of our classifer is simple. A multivariate linear discriminant analysis has been chosen, where the discriminant function can be expressed as follows [9]:

$$g(\mathbf{x}) = \mathbf{w}^{\mathbf{t}}\mathbf{x} + w_0 \tag{9}$$

where $\mathbf{w}$ is the weight vector and w_0 the bias or threshold weight. For a two-category classifier we will implement the following decision rule: decide ω_1 if $g(\mathbf{x}) > 0$ and ω_2 if $g(\mathbf{x}) \leq 0$.

III. Experiments and Results

A. Image preparation

All global MRI data were pre-processed to correct for intensity non-uniformity due to scanner variations [12], linearly registered into stereotaxic space and resampled onto a 1mm isotropic grid [5]. VOIs were defined on T1-weighted MR images with isotropic resolution of $1mm^3$. Initial testing was centered on the left medial temporal lobe (VOI of $55 \times 79 \times 68$ voxels). The extent of this volume captured the hippocampus and neighboring structures irrespective of normal inter- and intra-individual variability. The VOIs were then linearly registered unto a reference target (average of 152 ICBM subjects, see sec. III-B) to further reduce positional variations which would propagate as unwanted noise in the morphometric PCA modelling. Finally, VOIs were intensity-normalized with respect to the reference target for the same reason.

The following figures show grey-level sagittal images of the complete VOI near the hippocampus medial axis of two subjects, Subject Normal#2 in Fig. 1(a) and Subject TLE#1 in Fig. 1(b).

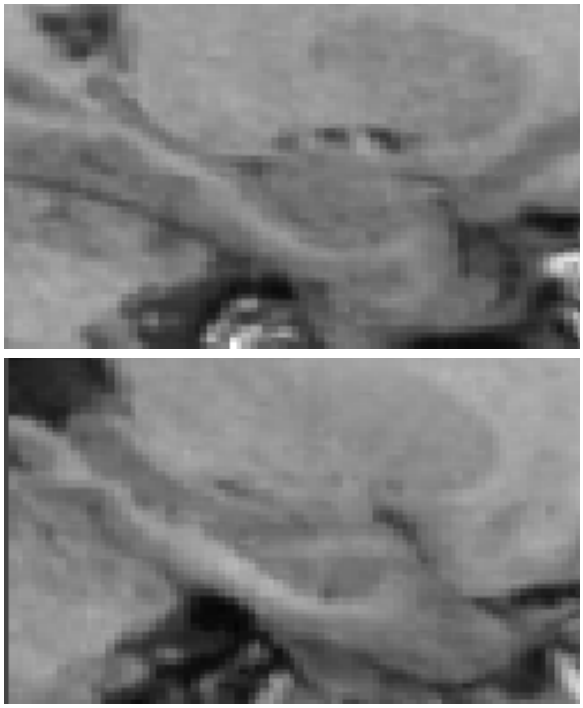

Fig. 1. (a) Normal subject #2 - Sagittal view through the medial axis of the left input VOI (b) TLE subject #1 - Sagittal view through the medial axis of the left input VOI

B. Creation of multi-dimensional grey-level space

The method described above was used to build a model of *left* MTL appearance. Figure 2 shows the number and cumulative weight r_k (see eq. 4) of eigenvectors for the Domain Definition set of 70 *normal* subjects taken from the International Consortium for Brain Mapping (ICBM) database [11]. We arbitrarily selected a threshold f of 97.5% which resulted in $t = 66$ eigenvectors being retained.

C. Linear Discriminant Analysis and Classification

In order to build our classifer we selected an additional 20 normal subjects and 20 confirmed TLE subjects with known atrophy of structures in the MTL as measured by one of the authors (N.B.). On the basis of clinical tests and EEG it was determined that 10 of those were predominantly *left* TLE and the remaining *right* TLE patients. The groups were matched for age and handedness. Prior probabilities for each state of nature ω were then equal, $p_{\omega(1,2)} = 0.5$.

Fig. 3 displays the position information for normal and TLE data sets along PC # 2 and 10. In these two examples one can readily see that there exists sufficient discrimination between the two probability density functions to allow classification.

The results from our multivariate linear discriminant analysis (LDA), using different numbers of eigenvectors T,

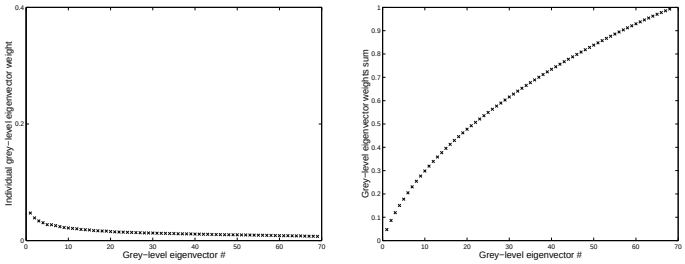

Fig. 2. Comparison of grey-level eigenvectors. (Left) Individual eigenvector weights as found in eq. 4 (Right) Eigenvector weights sum for the Domain Definition set. It is important to note that the large number of eigenvectors is a direct consequence of their expressing the variations in the difference from the mean element, and not the elements themselves. Recall that $p = N-1$ (N = 70) for this experiment and that for $f = 97.5\%$, $t = 66$ eigenvectors will be retained.

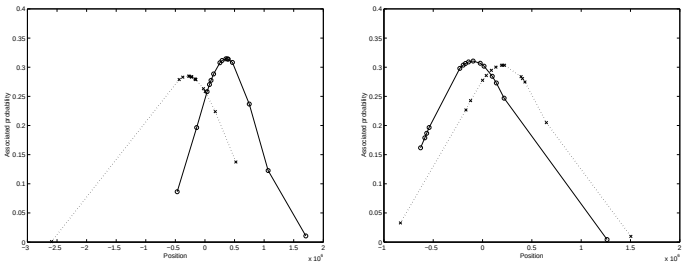

Fig. 3. Plot of position or eigencoordinates in Domain $\mathbf{G}^*$ for 15 Normal(x) and 15 TLE(o) subjects along PC axis 2 (left) and 10 (right)

are summarized in Table I and jacknifed analysis for the same conditions in Table II below. Following stepwise regression, we were able to obtain a total classification rate of 70% using only the first 10 PCs, with maximum discriminatory power concentrated in PC#10. Jacknife analysis for the same conditions lowers this total estimate to 68%. These rates jump to 100% accuracy in both types of analysis if we were to use all 66 eigenvectors available.

IV. Discussion

The formulation of this classification problem is simple and flexible, allowing a number of possible features to be used without extensive reengineering. Preliminary results indicate that the position information (eigencoordinates) of new data projected in a multi-dimensional grey-level Domain is sufficient to adequately discriminate between our two populations. The classification rates obtained here are comparable with those of volumetry obtained by one of the authors (N.B.).

A striking result is that a *left-sided* model was able to classify both *left and right-sided* TLE, which is commensurate with observations (see [4]) that the contra-lateral side is also affected by the disorder, albeit to a lesser degree. It is also important to note that the PCA technique as employed here requires no manual intervention other than the definition of the VOI, which is done once at the onset for the creation of the Domain $\mathbf{G}^*$. This is to be compared to volumetry, in which an expert neuroanatomist must man-

T = 10	Normals	TLE	% correct
Normals	14	6	70
TLE	6	14	70
Total	20	20	70
T = 39	Normals	TLE	% correct
Normals	15	5	75
TLE	5	15	75
Total	20	20	75
T = 66	Normals	TLE	% correct
Normals	20	0	100
TLE	0	20	100
Total	20	20	100

TABLE I

CLASSIFICATION MATRIX RESULTS FOR MULTIVARIATE LDA. T REPRESENTS THE NUMBER OF EIGENVECTORS RETAINED FOR THE ANALYSIS. TRUE CLASSIFICATION RESULTS ON THE NORMALS-NORMALS / TLE-TLE DIAGONAL.

T = 10	Normals	TLE	% correct
Normals	14	6	70
TLE	7	13	65
Total	21	19	68
T = 39	Normals	TLE	% correct
Normals	15	5	75
TLE	15	5	75
Total	20	20	75
T = 66	Normals	TLE	% correct
Normals	20	0	100
TLE	0	20	100
Total	20	20	100

TABLE II

JACKNIFED CLASSIFICATION MATRIX RESULTS FOR MULTIVARIATE LDA. T REPRESENTS THE NUMBER OF EIGENVECTORS RETAINED FOR THE ANALYSIS.TRUE CLASSIFICATION RESULTS ON THE NORMALS-NORMALS / TLE-TLE DIAGONAL.

ually delineate the ill-defined contours of structures of interest such as the HC, for a segmentation time of 2 hours per side per subject.

The relatively small number of subjects, compared to the number of eigenvectors available, preclude larger conclusions on the statistical significance of these results. Yet, it holds significant promise for the future. Future directions for our work will include: (a) include more data in the training and classification sets; (b) include non-linear registration of the training and classification VOIs to further reduce anatomical variability; (c) identification of the anatomical and pathological importance of the Principal Components holding maximum discriminatory power; and (d) factor analysis. It is also our hope that this classifier will be sufficiently robust to lateralize TLE into determining which of the two (left or right) MTL is most affected. Most likely this will imply the creation of a left and right-sided grey-level model and subsequent hierarchical classification.

V. Conclusion

The underlying assumption for this work is that there exists sufficient information in the grey-level intensity VOI of normal and abnormal subjects to be used for classification of normal and TLE patients. Hence, an appearance-based approach is proposed to extract features of interest from the images. The feature vector which we use corresponds to the eigencoordinates of our training data into multi-dimensional spaces formed by Principal Components of a grey-level linear model for this VOI. Preliminary results indicate that this technique can be highly successful. The ability to classify TLE without the need for explicit segmentation, and thus simply based on the appearance of MR images, would improve the current procedures of diagnostic as it is automated and objective.

Acknowledgments

Fonds pour les Chercheurs et l'Aide à la Recherche (Government of Québec) and ICBM.

References

[1] N. Bernasconi, A. Bernasconi, F. Andermann, F. dubeau, W. Feindel, and D. Reutens. Entorhinal cortex in temporal lobe epilepsy: a quantitative mri study. *Neurology*, 52(9):1870–1876, 1999.

[2] N. Bernasconi, A. Bernasconi, z. Caramanos, F. Andermann, F. Dubeau, and D. Arnold. Morphometric mri analysis of the parahippocampal region in temporal lobe epilepsy. *Ann N Y Acad Sci*, 911:495–500, 2000.

[3] E. Bertram. Functional anatomy of spontaneous seizures in a rat model of limbic epilepsy. *Epilepsia*, 38(1):95–105, 1997.

[4] F. Cendes, Z. Caramanos, F. Andermann, F. Dubeau, and D. Arnold. Proton magnetic resonance spectroscopic imaging and magnetic resonance imaging volumetry in the lateralization of temporal lobe epilepsy. *Ann Neurology*, 42:737–746, 1997.

[5] D. Collins, C. Holmes, T. Peters, and A. Evans. Automatic 3D Model-Based Neuroanatomical Segmentation. *Human Brain Mapping*, 3:190–208, 1995.

[6] T. Cootes, G. Edwards, and C. Taylor. Active Appearance Models. In *Proceedings of the European Conference on Computer Vision*, pages 484–498. ECCV, Verlag, 1998.

[7] J. Csernansky, S. Joshi, L. Wang, J. Haller, M. Gado, J. Miller, U. Grenander, and M. Miller. Hippocampal morphometry in schizophrenia by high dimensional brain mapping. In *Proceedings of the National Academy of Sciences*, volume 95, pages 11406–11411, 1998.

[8] S. Duchesne, J. Pruessner, and D. Collins. Appearance-based modelling and segmentation of the hippocampus from MR images. In *Proceedings of the 23rd Annual Conference of the IEEE Engineering in Medicine and Biology Society*, 2001.

[9] R. Duda, P. Hart, and D. Stork. *Pattern Classification*. Wiley-Interscience, 2nd edition, 2001.

[10] S. Joshi, S. Pizer, P. Fletcher, A. Thall, and G. Tracton. Multi-scale 3D Deformable Model Segmentation Based on Medial Description. In *Proceedings of the Information Processing in Medical Imaging Conference*, pages 64–77. IPMI, Springer, 2001.

[11] J. Mazziotta, A. Toga, A. Evans, P. Fox, and J. Lancaster. A probabilistic atlas of the human brain: Theory and rationale for its development. *NeuroImage*, 2:89–101, 1995.

[12] J. Sled, A. Zijdenbos, and A. Evans. A nonparametric method for automatic correction of intensity nonuniformity in mri data. *IEEE Transactions on Medical Imaging*, 17:87–97, 1998.

[13] M. Styner and G. Gerig. Medial Models incorporating object variability for 3D shape analysis. In *Proceedings of the Information Processing in Medical Imaging Conference*, pages 502–516. IPMI, Springer, 2001.